Elasticity of Stiff Polymer Networks

Jan Wilhelm and Erwin Frey

Hahn-Meitner-Institut, Abteilung Theorie, Glienicker Strasse 100, D-14109 Berlin, Germany
Fachbereich Physik, Freie Universität Berlin, Arnimallee 14, D-14195 Berlin, Germany

(Received 31 March 2003; published 5 September 2003)

We study the elasticity of a two-dimensional random network of rigid rods ("Mikado model"). The essential features incorporated into the model are the anisotropic elasticity of the rods and the random geometry of the network. We show that there are three distinct scaling regimes, characterized by two distinct length scales on the elastic backbone. In addition to a critical rigidity percolation region and a homogeneously elastic regime we find a novel intermediate scaling regime, where the elasticity is dominated by bending deformations.

DOI: 10.1103/PhysRevLett.91.108103 PACS numbers: 87.16.Ka, 62.20.Dc, 82.35.Pq

The elasticity of cells is governed by the cytoskeleton, a partially cross-linked network of relatively stiff filaments forming a several 100 nm thick shell called the actin cortex [1]. While the statistical properties of single cytoskeletal filaments are by now relatively well understood [2,3], theoretical concepts for the elasticity of stiff polymer networks are still evolving. One major open question is how stresses and strains are transmitted in such networks. In synthetic gels formed by rather flexible chain molecules the response to macroscopic external forces is — on the level of single filaments — isotropic and entropic in origin. It is generally believed that macroscopic stresses are transmitted in such a way that local deformations within the network stay affine, i.e., that the end-to-end distance of individual filaments follows the macroscopic shear deformation [4]. In contrast, the building blocks of the actin cortex are semiflexible polymers, whose hallmark is an extremely long persistence length ℓ_p comparable to the total contour length ℓ. As a consequence, the response of such stiff polymers to external forces shows a pronounced anisotropy [5]. Consider a semiflexible polymer with one end clamped at a fixed orientation. When forces are applied at the other end transverse to the tangent vector at the clamped end, the response may be characterized by a transverse spring coefficient $k_\perp(\ell) = 3\kappa/\ell^3$ proportional to the bending modulus κ. Whereas this response is of purely mechanical origin, the linear response to longitudinal forces is due to the presence of thermally excited undulations which make the average end-to-end distance of the polymer shorter than its contour length. The corresponding effective spring coefficient $k_\parallel(\ell) = 6\kappa^2/(k_B T \ell^4)$ is proportional to κ^2/T indicating the breakdown of linear response for very stiff filaments [2]. In a typical network one expects the distance between cross-links ℓ_c to be much smaller than the persistence length and filament length. Hence we have $k_\parallel(\ell_c)/k_\perp(\ell_c) = 2\ell_p/\ell_c \gg 1$, i.e., the elastic response of the filaments is indeed highly anisotropic.

The anisotropic elastic properties of individual filaments suggests that the macroscopic elasticity of networks depend on the number of cross-links and the density of filaments, but also on the geometry and architecture of the network. For some very regular networks such as a triangular lattice the longitudinal spring coefficient $k_\parallel$ dominates the macroscopic moduli [6] since the network cannot be strained without a change of the end-to-end distance of individual polymers. In other regular network architectures, the softer bending modes would be dominant [7]. Naturally, this will lead to a very different prediction for the elastic modulus of the network. It is not at all obvious what type of network geometry (elongation dominated versus bending dominated) is relevant in less ideal structures with a significant amount of disorder as found in typical cytoskeletal networks.

As a first step towards understanding the elasticity of stiff polymer networks we consider a two-dimensional model defined as follows (see Fig. 1). We generate the random network by placing N linelike objects of equal length ℓ on a plane with area $A = L^2$ such that both position and orientation of the filaments are uniformly randomly distributed. Periodic boundary conditions in both directions are used. Upon increasing the line density $\rho = N\ell/A$ there is a critical threshold ρ_c for geometric percolation [8]. Numerical simulations [9] show that the correlation length $\xi \sim (\rho - \rho_c)^{-\nu}$ of the incipient infinite percolation cluster scales with a critical exponent $\nu = 4/3$, identical to the value obtained for random site percolation on a lattice [10]. Transport of scalar quantities like the conductivity is also in the same universality class as lattice models [11]. In order to study the transport of nonscalar quantities such as shear stress we need to specify how forces are transmitted between the building blocks of the network. In our Mikado model the building blocks are homogeneous elastic rods characterized by a Young modulus E and a circular cross section of radius r. Wherever two rods intersect, they are connected by a cross-link with zero extensibility. In the cytoskeleton one finds a variety of linker proteins with a range of mechanical properties [12]. Here we restrict ourselves to cross-links that either fix the relative orientation of the rods ("stiff cross-links") or allow free rotation ("free hinges"). Similar to thermally fluctuating semiflexible

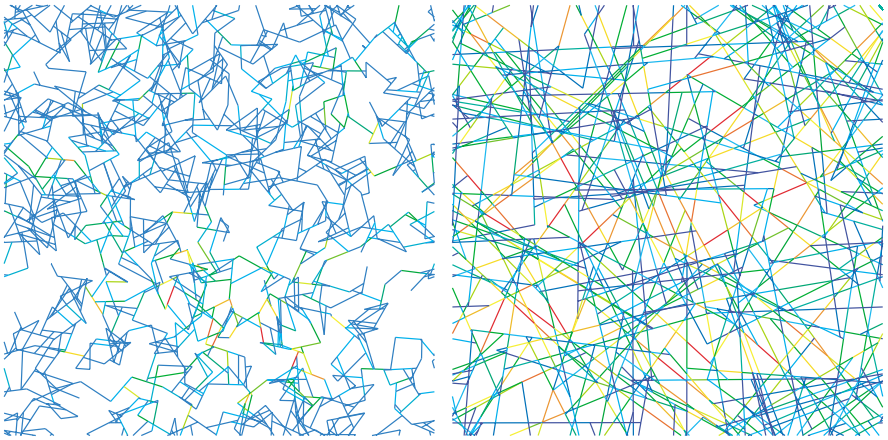

FIG. 1 (color). Typical networks at low and high density. Dangling bonds, not contributing to the elasticity, have been cut off. The stress distribution is shown in false colors; the load on a filament increases from blue to red. The left picture is for $\rho = 10$, system size $L = 10$, and an aspect ratio $\alpha = 0.0001$. 99.99% of the strain energy is stored in bending modes. In contrast, the right picture shows a network for $\rho = 50$, $L = 2$, and $\alpha = 0.01$, where only 5% of the strain energy is in bending modes; the remainder is stored in compression modes. For the choice of units see the main text.

polymers, the elastic response of a stick segment between two neighboring cross-links is characterized by length dependent force constants for compression or elongation, $k_{\mathrm{comp}}(\ell_c) = \pi r^2 E/\ell_c$, and bending, $k_{\mathrm{bend}}(\ell_c) = k_\perp(\ell_c) = (3/4)\pi r^4 E/\ell_c^3$. The distance between two cross-links ℓ_c shows a Poissonian distribution, where the average distance of cross-links along a filament scales as the inverse of the line density, $\bar{\ell}_c = \pi/\rho$ [8]. While this is a purely mechanical model that does not exhibit the temperature dependent longitudinal linear response force constant $k_\parallel$ of thermally fluctuating semiflexible polymers given above, it still captures the essential feature that the compressional stiffness is much larger than the bending stiffness $k_{\mathrm{comp}}(\ell_c)/k_{\mathrm{bend}}(\ell_c) = (4/3)\ell_c^2/r^2 \gg 1$ for typical densities of the network. It does not account for steric effects due to thermal fluctuations of the filaments, which give rise to the plateau modulus in solutions [13].

Consider the ground state energy of the network as a function of the deviations of the positions of all cross-links and the rod orientations at the cross-links from their initial values. For small deformations of the network, this function can be approximated by a quadratic form that vanishes for vanishing deviations, as — by construction — the undeformed network is not prestressed. The matrix representing the quadratic form can be computed from the network geometry and the elastic constants. Note that this linearized model cannot account for the effect of buckling instabilities appearing for finite deformations. To analyze the elastic properties of the model network, a shear deformation respecting the periodic boundary conditions is enforced by demanding that corresponding points on the left and right boundary of the simulation cell undergo equal displacements while the displacements of corresponding points on the upper and lower boundary of the cell must agree vertically but differ horizontally by a distance $\Delta = \gamma L$, where γ is the shear strain. The orientation of the rods at corresponding points on the boundary are required to be equal. The remaining degrees of freedom are then allowed to relax, i.e., the harmonic approximation to the energy of the network is minimized in the presence of the constraints. The derivative of the resulting energy of the deformed state with respect to the strain γ is proportional to the shear modulus. This reduces the determination of the modulus of a given network to the solution of a linear equation. However, for interesting parameters (thin rods), the problem is numerically highly unstable as we are searching for the lowest point of a complicated high-dimensional valley with extremely steep slopes but hardly varying base altitude. The results presented below were obtained using the commercially available finite element solver Nastran by MSC Software.

In the following discussion we choose the rod length ℓ as unit of length and κ/ℓ^3 as unit for the elastic modulus. Then the independent parameters are density ρ, system size L and aspect ratio $\alpha = r/\ell$ of the rods. Note that the latter is a measure of the relative magnitude of compressional to bending stiffness.

We start with an analysis of the elasticity close to the percolation threshold. For stiff cross-links we find that the percolation threshold is the same for rigidity as for connectivity percolation, $\rho_c = 5.71$. For free hinges a higher line density $\rho_c = 6.7$ is needed for the network to become rigid. This agrees well with recent results, $\rho_c = 6.68$, for stiff fiber networks [14], where the cross-links are fixed in space but the angles between the fibers can vary. In both cases, we find that the shear modulus G vanishes like $G \sim (\rho - \rho_c)^\mu$ as the line density approaches the critical value ρ_c. For our numerical analysis with finite systems we expect the shear modulus to obey the following finite size scaling law

$$G = L^{-\mu/\nu} h(L/\xi), \tag{1}$$

where the scaling function behaves as $h(x) \sim x^{\mu/\nu}$ and $h(x) \sim 1$ for large and small values of $x = L/\xi$, respectively. Figure 2 shows that the data collapse works very well for densities ranging from values close to ρ_c up to $\rho \approx 20$. For the data shown, L ranges from 2 to 30. For larger densities, systematic deviations are clearly visible, indicating that the length scale $r = \alpha\ell$ becomes relevant here. We will discuss the behavior in the high density regime in more detail below. We get the best data collapse

in the critical region if we choose the values 2.4 ± 0.2 and 2.3 ± 0.2 for the critical exponent μ/ν in the case of stiff cross-links and free hinges, respectively. Since the difference between the exponents is within the statistical error, we can make no definite conclusion whether networks with free hinges and stiff cross-links belong to different universality classes. The rigidity exponent $\mu \approx 3.15 \pm 0.2$ is significantly lower than in other classes of continuum percolation models, such as the "Swiss-cheese model," where $\mu \approx 5$ [15,16]. It is also lower than the value $\mu \approx 4$ for lattice models with bond-bending forces [10,17]. Hence it seems likely that the Mikado model constitutes a new universality class for rigidity percolation. Similar results have been found in Ref. [18].

We now come back to the systematic deviations from the scaling law, Eq. (1), at densities above $\rho \approx 20$. To understand these better, let us have a closer look at the shear modulus as a function of $r = \alpha\ell$ for densities not too close to the percolation threshold. In this regime the shear modulus becomes independent of system size for moderately large systems; for the following results we have chosen systems satisfying $L/\xi \geq 200$. Figure 3 shows the shear modulus as a function of α for a series of densities; we have communicated a preliminary version of these data in Ref. [19]. Note that $k_{\mathrm{bend}}(\ell)$ is effectively kept constant since we are measuring all elastic constants in units of κ/ℓ^3. There are two strikingly different regimes. For high densities and/or thick rods ($\alpha \gtrsim 0.1$), where compressional stiffness is lower or comparable to the bending stiffness (lower right part of Fig. 3), the shear modulus scales linearly with the filament compressional modulus and the number of filaments per unit area, $G \sim (\rho - \rho_c)\alpha^{-2}$. Such a linear regime has also been found in a series of studies on random fiber networks [20]. It is by now well established that the elastic modulus in this regime can be described quantitatively in terms of effective medium models [21]. Hence, in the high line density regime the network behaves as a homogeneously elastic medium, dominated by the compressional modulus of the individual filaments. As a consequence, local deformations follow a macroscopic shear in an affine way. This has to be contrasted with the elastic behavior for slender rods with low aspect ratios ($\alpha \approx 10^{-5}$ for the higher densities), where bending becomes the softer mode. We find an extended plateau region, which broadens significantly with lowering the line density, where the shear modulus becomes completely independent of $k_{\mathrm{comp}}(\ell) \sim \alpha^{-2} k_{\mathrm{bend}}(\ell)$ [19]. This strongly suggests that in this regime the macroscopic elasticity of the network is dominated by the bending stiffness of the filaments. This conclusion is corroborated by the observation that almost all of the energy stored in the deformed network is accounted for by transverse deformation of the rods (compare Fig. 1). Another remarkable feature of the plateau regime is the strong dependence of the shear modulus on line density. We find $G \sim (\rho - \rho_c)^{\mu'}$ with a rather large exponent $\mu' \approx 6.7$. Figure 3 suggests the crossover scaling ansatz

$$G = (\rho - \rho_c)^{\mu'} g[\alpha(\rho - \rho_c)^{\nu'}] = \xi'^{-\mu'/\nu'} \tilde{g}(\alpha/\xi'), \quad (2)$$

where we have defined a new length scale $\xi' \sim (\rho - \rho_c)^{-\nu'}$. For this ansatz to reduce to the modulus expected in the affine region, the scaling function $g(x)$ needs to scale as $g(x) \sim x^{-2}$ for $x \gg 1$ and the exponents need to obey the scaling relation $\mu' = 2\nu' + 1$. In the plateau regime, $g(x)$ is expected to be constant. As shown in Fig. 4, we obtain an excellent scaling collapse for over almost 8 orders of magnitude in the scaling variable $x = \alpha/\xi'$ using $\nu' = 2.83$ or equivalently $\mu' = 6.67$ and the critical line density $\rho_c \approx 5.71$ associated with connectivity percolation. Additionally, the scaling function $g(x)$

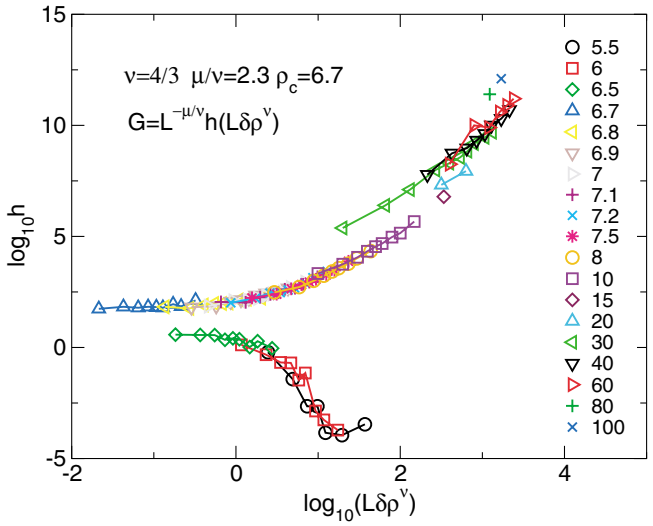

FIG. 2 (color). Double logarithmic plot of the scaling function $h(x)$ for the shear modulus of the "Mikado model" with free hinges as a function of $x = L|\delta\rho|^{\nu}$ with $\delta\rho = \rho - \rho_c$ for a series of densities ρ indicated in the graph. Note that for finite systems the shear modulus is also nonzero below ρ_c (lower branch in the plot). The corresponding plot for stiff hinges is similar, but exhibits a different $\rho_c = 5.71$ (see text).

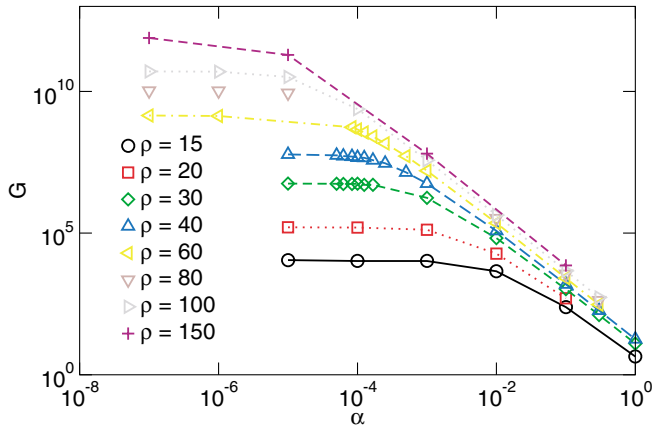

FIG. 3 (color). Double logarithmic plot of the shear modulus G as a function of α for fixed $k_{\mathrm{bend}}(\ell)$. Data shown for free hinges.

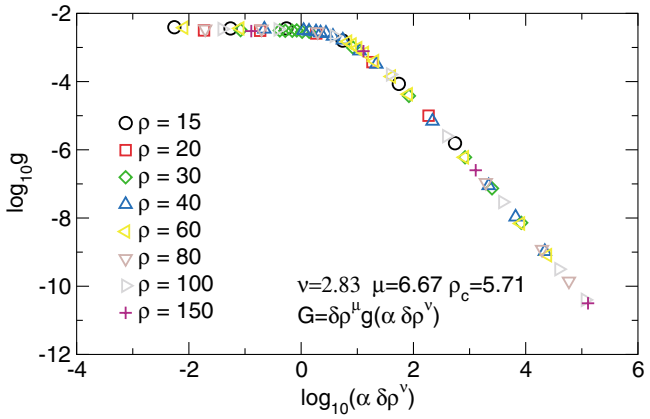

FIG. 4 (color). Scaling plot of the shear modulus for free hinges for a series of densities above $\rho = 15$ indicated in the graph (same data as in Fig. 3). Data collapse to the crossover scaling form, Eq. (2), is obtained with $\nu' = 2.83$. Note that here and in all other figures the unit of length is ℓ and the unit of the shear modulus G is κ/ℓ^3.

displays the expected behavior. Meeting both of these requirements is highly nontrivial, and gives strong evidence for the anomalous scaling law in Eq. (2).

The existence of such a broad scaling regime far from the percolation threshold is a surprising and intriguing feature of stiff polymer networks. Its physical origin is distinct from the critical scaling regime, and governed by a new length scale ξ'. While the geometrical significance of ξ' is yet unclear, one may speculate that the anomalous scaling behavior is a subtle consequence of the interplay between quenched randomness of the network structure and long-range correlation effects induced by the stiffness of the filaments. An immediate consequence of the scaling form, Eq. (2), is the existence of a crossover line density ρ_{cross} scaling as $\ell\rho_{\text{cross}} \sim \alpha^{-1/\nu'}$, where we have reintroduced units of length ℓ. This implies that increasing filament length at constant line density drives the system towards the affine regime, in accord with Ref. [18].

While these results for an idealized two-dimensional model are certainly not straightforwardly applicable to three-dimensional cytoskeletal networks, one may still try to get an idea of the scales involved. We expect that network densities can be compared roughly by using the average distance ℓ_c between intersections as a measure: A cytoskeletal network might have $\ell_c \approx 0.1\ \mu$m with filament lengths of $2\ \mu$m and filament radii of 4 nm. These values correspond to a two-dimensional line density of $\rho \approx 20$ and an aspect ratio of $\alpha \approx 0.002$, which would place a typical actin network in the bending dominated intermediate regime at $T = 0$. For $T > 0$, a faithful treatment of thermal fluctuations of the network would require the inclusion of the polymer configuration as additional degrees of freedom. However, in a first approximation, the fluctuations of the polymers between cross-links could be represented by replacing the longitudinal force constant k_{comp} used in the present analysis by the thermal linear response coefficient $k_{\|}$ discussed in the introduction augmented by numerical prefactors to reflect the local boundary conditions. As the dependence of $k_{\|}$ on the random distance between cross-links is quite different from that of k_{comp}, this may well lead to different scaling behavior. Additional contributions to the modulus are expected when thermal fluctuation of the cross-link positions are taken into account [22]. Understanding the full complexity of cytoskeletal networks certainly merits further theoretical and experimental work. Future investigations may among many other questions want to address three-dimensional systems, polydispersity, thermal fluctuations, or even the kinetics of the cross-linking molecules.

We thank M. Alava and K. Kroy for discussions, and P. Benetatos for a critical reading of the manuscript.

[1] B. Alberts *et al.*, *Molecular Biology of the Cell* (Garland Publishers, New York, 1994), 3rd ed.
[2] J. Wilhelm and E. Frey, Phys. Rev. Lett. **77**, 2581 (1996).
[3] L. LeGoff, O. Hallatschek, E. Frey, and F. Amblard, Phys. Rev. Lett. **89**, 258101 (2002).
[4] M. Doi and S. F. Edwards, *The Theory of Polymer Dynamics* (Clarendon Press, Oxford, 1986).
[5] K. Kroy and E. Frey, Phys. Rev. Lett. **77**, 306 (1996).
[6] F. MacKintosh, J. Käs, and P. Janmey, Phys. Rev. Lett. **75**, 4425 (1995).
[7] R. Satcher and C. Dewey, Biophys. J. **71**, 109 (1996).
[8] G. Pike and C. Seager, Phys. Rev. B **10**, 1421 (1974).
[9] Y. Leroyer and E. Pommiers, Phys. Rev. B **50**, 2795 (1994).
[10] D. Stauffer and A. Aharony, *Introduction to Percolation Theory* (Taylor & Francis, London, 1994), 2nd ed.
[11] I. Balberg, N. Binenbaum, and N. Wagner, Phys. Rev. Lett. **52**, 1465 (1984).
[12] L. Limozin and E. Sackmann, Phys. Rev. Lett. **89**, 168103 (2002).
[13] B. Hinner *et al.*, Phys. Rev. Lett. **81**, 2614 (1998).
[14] M. Latva-Kokko and J. Timonen, Phys. Rev. E **64**, 066117 (2001).
[15] S. Feng, B. I. Halperin, and P. N. Sen, Phys. Rev. B **35**, 197 (1987).
[16] L. Benguigui, Phys. Rev. B **34**, 8176 (1986).
[17] S. Arbabi and M. Sahimi, Phys. Rev. B **47**, 703 (1993).
[18] D. A. Head, A. J. Levine, and F. C. MacKintosh, Phys. Rev. Lett. (to be published).
[19] E. Frey, K. Kroy, J. Wilhelm, and E. Sackmann, in *Dynamical Networks in Physics and Biology*, edited by G. Forgacs and D. Beysens (Springer-Verlag, Berlin, 1998).
[20] V. Räisänen, M. Alava, K. Niskanen, and R. Nieminen, J. Mater. Res. **12**, 2725 (1997).
[21] J. Åström *et al.*, Phys. Rev. E **61**, 5550 (2000).
[22] M. Plischke and B. Joós, Phys. Rev. Lett. **80**, 4907 (1998).